Resonant field enhancement by a finite-size periodic array of surface scatterers

2001 J. Phys.: Condens. Matter 13 3001

(http://iopscience.iop.org/0953-8984/13/13/313)

INSTITUTE OF PHYSICS PUBLISHING JOURNAL OF PHYSICS: CONDENSED MATTER

J. Phys.: Condens. Matter **13** (2001) 3001–3010 www.iop.org/Journals/cm PII: S0953-8984(01)20573-6

Resonant field enhancement by a finite-size periodic array of surface scatterers

Mufei Xiao[1,3] **and Sergey I Bozhevolnyi**[2]

[1] Centro de Ciencias de la Materia Condensada, Universidad Nacional Autonoma de México, Apartado Postal 2681, Ensenada, CP 22800, Baja California, Mexico
[2] Institute of Physics, Aalborg University, Pontoppidanstræde 103, DK-9220 Aalborg Øst, Denmark

E-mail: mufei@ccmc.unam.mx

Received 2 January 2001

Abstract

Using a microscopic point-dipole description of light scattering by surface particles, we investigate evolution of the self-consistent field intensity distribution above a finite-size hexagonal array of surface scatterers when changing the light wavelength. It is found that, for sufficiently strong scatterers, the wavelength dependences of the maximum field intensity exhibit narrow resonances, at which the field is significantly enhanced. We investigate the influence of the system parameters, such as the polarizability of scatterers, wavelength, polarization and angle of incidence of the incoming wave, on the self-consistent field intensity distributions at resonance. Near-field optical probing of the resonant field intensity patterns is also considered.

1. Introduction

Light scattering by periodic 2D and 3D dielectric structures has been intensively studied in the context of photonic band gap (PBG) structures during the last 10 years [1]. If the contrast of the periodic modulation of the dielectric constant is sufficiently large, Bragg scattering in such a medium can significantly influence the nature of photonic modes resulting eventually in the PBG effect. A finite-size periodic structure of scatterers, which is placed on a substrate and illuminated by a totally internally reflected (TIR) wave, is in many respects similar to but also rather different from PBG structures [2]. Such a structure being periodical in the surface plane, i.e. in two dimensions, and confined in the direction perpendicular to it scatters the incoming field in three dimensions. Therefore, one can hardly determine its transmission and reflection characteristics and identify allowed or forbidden frequency regions (i.e. determine the PBG). On the other hand, as in PBG structures, strong light scattering can occur in a finite-size periodic structure of surface scatterers (FSPSSS), e.g. under TIR illumination, so that the scattered field is significantly enhanced near an FSPSSS [2].

[3] Corresponding author: Dr Mufei Xiao, CCMC–UNAM, PO Box 439036, San Ysidro, CA, USA.

0953-8984/01/133001+10$30.00

Light scattering by a FSPSSS can be enhanced due to the structure periodicity leading to constructive interference of waves scattered by individual scatterers. Such an enhancement would be most pronounced for the FSPSSS containing a relatively large number of scatterers separated with the spatial period of the order of the wavelength of light. Consequently, the appropriate consideration should include retardation effects, i.e. the electrostatic approximation that is often employed in near-field optics [3] and optics of fractal clusters [4] can no longer be used. Taking also into account that the description of strong (resonant) multiple scattering calls for the usage of a self-consistent approach [5], one realizes that the study of light scattering by a FSPSSS (including the search for the resonant field enhancement) is by no means an easy task and that one can hardly avoid making some simplifications. The main approximation we used was that the surface scatterers were treated as (point) electric (isotropic) dipoles with wavelength independent polarizabilities. This allowed us to make a clear distinction between the phenomenon of light enhancement in a certain *configuration* of an *ensemble* of scatterers and the field enhancement in a certain *wavelength* range due to the (plasmon and/or Mie) resonances in the polarizability of an *individual* scatterer [6].

In this paper we consider multiple light scattering by a periodic array of identical spherical particles placed on a substrate and illuminated from the side of the substrate by a totally internally reflected wave. It is demonstrated that, for certain combinations of light wavelengths, array periods and sphere radii, the total (self-consistent) field established in the process of strong multiple scattering by a FSPSSS can be *resonantly* enhanced. We investigate and report main features of this new scattering phenomenon. Furthermore, near-field optical probing of the field intensity distributions at resonance is also discussed.

2. Main formulae

The configuration of the considered FSPSSS is shown in figure 1. Light scattering by spherical scatterers placed on the surface of the bulk was treated in the electric-dipole approximation [5, 7]. Within this microscopic formalism, the total electric field in the system is given by the following expression:

$$\boldsymbol{E}(\boldsymbol{r},\omega) = \boldsymbol{E}_{in}(\boldsymbol{r},\omega) - \mu_0\omega^2 \sum_{j=1}^{N} a_j(\omega)\boldsymbol{G}(\boldsymbol{r},\boldsymbol{r}_j,\omega)\cdot\boldsymbol{E}(\boldsymbol{r}_j,\omega) \tag{1}$$

where $\boldsymbol{E}_{in}(\boldsymbol{r},\omega)$ is the monochromatic incident field at the frequency ω, $\boldsymbol{G}(\boldsymbol{r},\boldsymbol{r}_j,\omega)$ is the appropriate field propagator and $\boldsymbol{E}(\boldsymbol{r}_j,\omega)$ is the self-consistent field at the site of the jth surface scatterer with the (dipolar) polarizability $\alpha_j(\omega)$. In the scattering system with an interface, the field propagator consists of direct and indirect parts [5]. We used the complete retarded form of the direct part of the field propagator $\boldsymbol{G}$, and the indirect part was approximated by the retarded direct propagator from the corresponding (mirror) image dipole [8], *viz.*,

$$\boldsymbol{G}(\boldsymbol{r},\boldsymbol{r}_j,\omega) = \boldsymbol{D}(\boldsymbol{r},\boldsymbol{r}_j,\omega) + \boldsymbol{D}(\boldsymbol{r},\boldsymbol{r}_{mj},\omega)\cdot\boldsymbol{M}(\omega)$$

$$\text{where}\quad \boldsymbol{M}(\omega) = \frac{\varepsilon_b(\omega)-1}{\varepsilon_b(\omega)+1}\begin{pmatrix} -1 & 0 & 0 \\ 0 & -1 & 0 \\ 0 & 0 & 1 \end{pmatrix} \tag{2}$$

$\boldsymbol{r}_{mj} = (x_j, y_j, -z_j)$ points to the image dipole, $\varepsilon_b(\omega)$ is the bulk dielectric constant, $\boldsymbol{D}(\boldsymbol{r},\boldsymbol{r}_j,\omega)$ is the (direct) field propagator (or dyadic Green's function) in free space:

$$\boldsymbol{D}(\boldsymbol{r},\boldsymbol{r}_j,\omega) = \frac{1}{4\pi}\left[\left(-\frac{1}{R} - \frac{\mathrm{i}c}{\omega R^2} + \frac{c^2}{\omega^2 R^3}\right)\boldsymbol{U} + \left(\frac{1}{R} + \frac{3\mathrm{i}c}{\omega R^2} - \frac{3c^2}{\omega^2 R^3}\right)\boldsymbol{e}_R\boldsymbol{e}_R\right]\exp(\mathrm{i}kR) \tag{3}$$

$R = |\boldsymbol{r} - \boldsymbol{r}_j|$, $\boldsymbol{e}_R = (\boldsymbol{r} - \boldsymbol{r}_j)/R$, $\boldsymbol{U}$ is the unit tensor and $k = \omega/c$ is the wavenumber of light in free space.

The incident field was considered in the form of a plane wave with the amplitude equal to 1 and having s- or p-polarization, i.e. with the electric field being polarized perpendicular to or in the plane of incidence. This wave was incident from the side of the substrate at the angle θ exceeding the critical angle (figure 1(a)), so that the surface spheres were illuminated by the evanescent field. Finally, the polarizability of a surface sphere was calculated in the long-wavelength electrostatic approximation via the sphere's radius a and its dielectric constant $\varepsilon_s(\omega)$:

$$\alpha(\omega) = 4\pi\varepsilon_0 a^3 \frac{\varepsilon_s(\omega) - 1}{\varepsilon_s(\omega) + 2}. \tag{4}$$

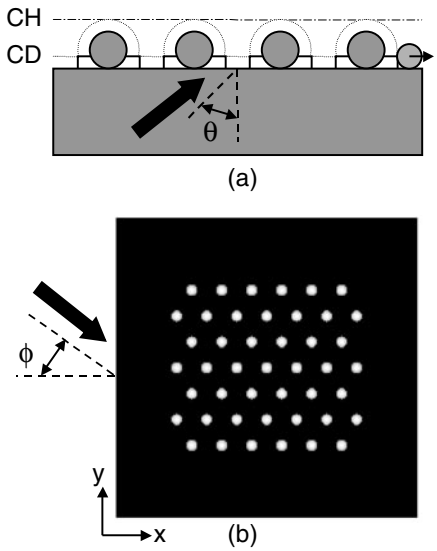

Figure 1. Geometry of the scattering system under consideration. (a) Cross section of a finite-size hexagonal array of 200 nm radius spherical scatterers illuminated by total internal reflection; (b) topographical image ($6 \times 6\ \mu\text{m}^2$) simulated with a 10 nm radius probe sphere.

The self-consistent field at the sites of the scatterers can be found by using their locations in turn as the observation point in equation (1) and solving the resulting set of equations with standard procedures of linear algebra [5]. The total self-consistent field established in the process of multiple scattering can then be determined at any point of the considered configuration. In our simulations, we have chosen to use frequency independent values of dielectric constants of the substrate and scatterers. This means that the results obtained for a particular scattering configuration can be applied to other configurations that have the same geometrical arrangement and the same ratios between the distances involved (including the radius of the surface spheres) and the light wavelength (see equations (1)–(4)). Actually, the variation in the sphere's dielectric constant ε_s can be compensated adjusting the radius a to keep the same value of the polarizability (equation (4)) as long as all other parameters are kept without changes.

3. Numerical results

First, we investigated the wavelength dependence (in the range of 500–750 nm) of the maximum of the self-consistent field intensity calculated above the hexagonal FSPSSS (with the spatial period of 600 nm) at the constant height (CH) of 211 nm from the substrate surface (figure 1(a)). The substrate with the dielectric constant $\varepsilon_b = 10$ illuminated by a TIR wave incident under the angle $\theta = 25^\circ$, two dielectric constants ($\varepsilon_s = 5$ and 10) of the surface spheres with the radius of 100 nm and three angles of incidence in the surface plane ($\phi = 0$, 30 and 45°) were used in these calculations (figure 2). Similar to what has been reported previously [2], we found that, in general, the field intensity is considerably enhanced in a large range of light wavelengths around 600 nm, i.e. around the value of the FSPSSS period. Note that the field intensity that would be observed at the same distance above a bare surface is ∼0.07 for the considered configuration.

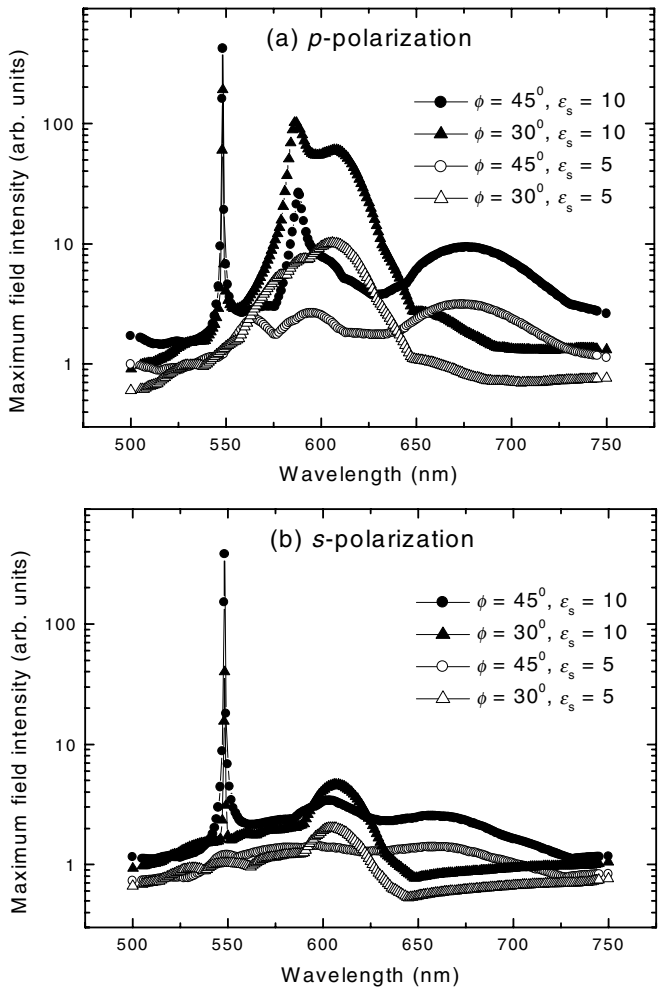

Figure 2. Wavelength dependences of the maximum of the field intensity calculated at the constant height of 211 nm from the substrate surface for different angles ϕ (figure 1(b)) and dielectric constants of scatterers illuminated with (a) p- and (b) s-polarized plane waves.

In addition to the overall field enhancement, we have also observed pronounced peaks in the wavelength dependences calculated for the scatterers with $\varepsilon_s = 10$ (figure 2). A very sharp (width ∼0.5 nm) and high peak has been found at the wavelength of 548.2 nm for all polarizations and angles ϕ, though the peak height was very different varying from 7 (for p-polarization and $\phi = 0^\circ$) to 1050 (for s-polarization and $\phi = 0^\circ$). A less pronounced peak has been found at the wavelength of ∼590 nm but only for p-polarization and with the position slightly dependent on the angle ϕ. Note that the wavelength dependences calculated for different dielectric constants are rather similar to each other so that, apart from some factor, the resonant peaks constitute the only difference between these dependences.

We attribute the appearance of these peaks to the transition (with the increase of the scatterers' polarizabilities) between the regimes of relatively weak and strong (resonant) multiple scattering. The same transition can be also realized by changing the radius of spherical scatterers (equation (4)). Calculating the intensity maximum as a function of *both* wavelength λ and radius a (with all other parameters being constant), one can determine the exact locations of these resonances (figure 3). Note that the maximum intensity can reach values that are four orders of magnitude larger than the incident field intensity. It should be stressed that the radius determining the scatterer's strength (polarizability) and the light wavelength determining the scattered field decay with the distance (equation (3)) are the most and *equally* important parameters of scattering system. This feature reflects the principal difference existing between these resonances and the (plasmon and/or Mie) resonances in the polarizability of individual scatterers.

Conceptually, the observed resonances are similar to the configurational resonances, though those were introduced for near-field interactions [5]. In our case, even in the absence of damping the heights of the resonance peaks are finite because of the retardation. Similar calculations for the dielectric constant of scatterers containing also an imaginary part showed that the resonance peaks became slightly shifted in wavelength and decreased in height. Representing the set of equations for the self-consistent field at the sites of the scatterers in a symbolic form, viz., $E = E_0 + FE$, one realizes that the resonance condition is given by the characteristic equation $\mathrm{Re}\{\det|U - F|\} = 0$ [5]. It is clear that, for a system containing a finite number of scatterers, this condition can be satisfied only for a discreet set of system parameters.

The distribution of the self-consistent field at resonance is determined by the configuration of the scattering system and stable with respect to the incident field. The field intensity distributions, which were calculated for s- and p-polarizations of the incident field at 548.2 nm, are indeed similar to each other for all angles ϕ except for the case of the p-polarized wave incident along the x-axis (figure 4). This exception is explained by the circumstance that the main contribution to the resonant field intensity comes from the y-component of the field. Since the y-component of the incident field is exactly zero for the p-polarized wave incident at ($\phi = 0^\circ$, the resonant field cannot be excited in this configuration, and therefore the resulting field intensity is significantly smaller and distributed differently than in other cases (cf figures 4(a), 4(d) and 4(c)). Note that the resonant field enhancement is tightly bound to the sample surface (cf figures 4(a) and 4(b)) indicating that the evanescent field components play a crucial role in this resonance.

We have also calculated the self-consistent field intensity at the site of a probe sphere ($\varepsilon_p = 2.5$, radius $a_p = 10$ nm) scanned over the sample surface at the constant distance (CD) of 1nm (figure 1(a)). The idea was to simulate a near-field optical image of the field intensity distribution [7] and to identify the locations of high field intensities near the actual sample surface. The corresponding topographical image is shown in figure 1(b), and the simulated images for the wavelength of 548.2 nm are shown in figure 5. These images are rather different from the field intensity distributions calculated in CH mode (cf figures 4 and 5). The analysis of

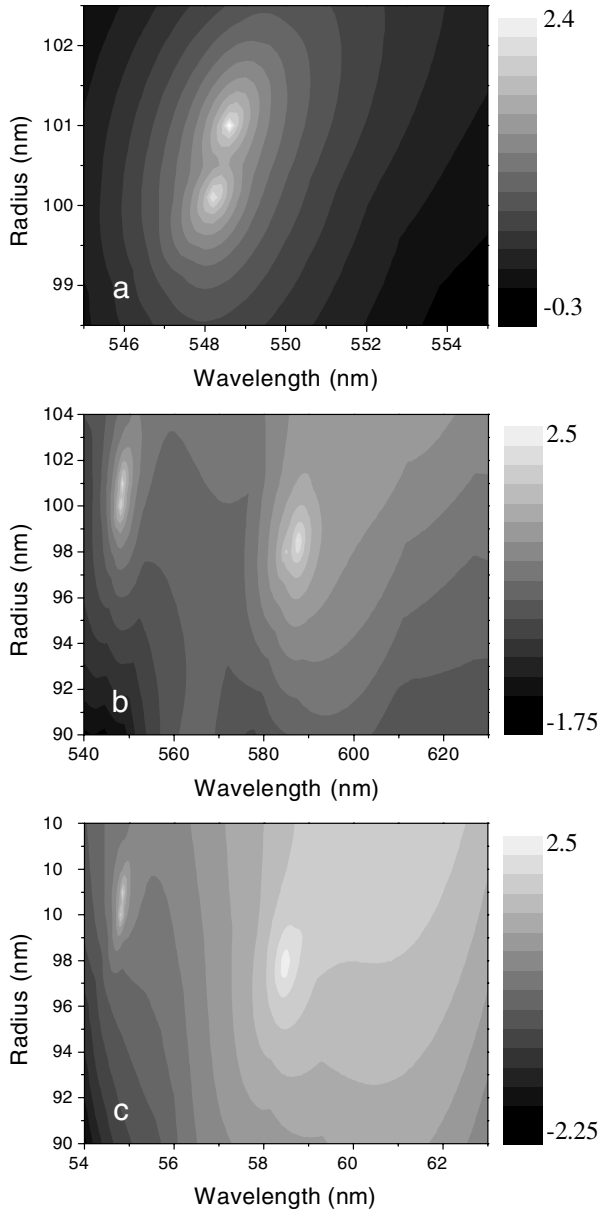

Figure 3. Grey-scale representations of the double logarithm of the maximum of the field intensity, i.e., $\ln[\ln(I)]$, calculated at the constant height of 211 nm from the substrate surface for different angles: $\phi = 45^\circ$ (a), (b) and 30° (c) and polarizations of the incident wave: (a) s- and (b), (c) p-polarization.

the observed differences is quite intricate and will be presented in detail elsewhere. The main reasons are the perturbation (by the probe sphere) of the self-consistent field at resonance [9] and the fact that the actual surface of mapping the field intensity in CD mode is very different from the plane used for calculations in CH mode (with their separation being up to 200 nm). It should be noted also that the images obtained for $\phi = 30$ and 45° and two polarizations were

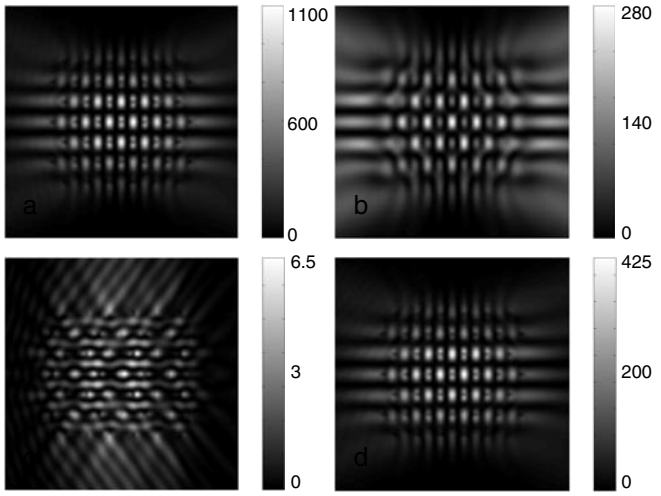

Figure 4. Linear grey-scale representations ($6 \times 6\ \mu m^2$) of the field ($\lambda = 548.2$ nm) intensity calculated at the constant height of (a), (c), (d) 211 and (b) 500 nm from the substrate surface for (a), (b) s-polarization and $\phi = 0^\circ$, (c) p-polarization and $\phi = 0^\circ$ and (d) p-polarization and $\phi = 45^\circ$.

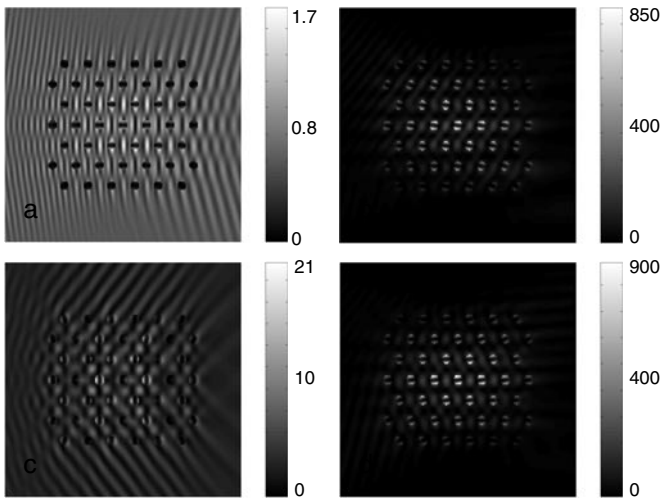

Figure 5. Linear grey-scale representations ($6 \times 6\ \mu m^2$) of the field ($\lambda = 548.2$ nm) intensity calculated at the site of the probe sphere scanned at the constant distance of 1 nm from the surface for (a), (b) s- and (c), (d) p-polarized wave incident at $\phi =$ (a), (c) 0° and (b), (d) 45°.

found quite similar to each other and with the strongest field intensities located on both sides of surface scatterers along the y-axis (cf figures 5(b) and 5(d)). The latter feature is explained by the resonant enhancement of the y-component of the field at the site of the scatterers.

The resonant intensity enhancement at $\sim$590 nm with a p-polarized incident beam (figures 2(a), 3(b) and 3(c)) is related to the enhancement of the z-component of the field (normal to the surface plane). The resonance peaks for different angles ϕ turned out to be slightly displaced and the corresponding intensity distributions different (figure 6). Judging from the intensity distributions, it is plausible to suggest that these resonances are due to the resonance

interaction between resonantly excited hexagonal clusters of scatterers in the FSPSSS. The distance between neighbour (elementary) clusters depends upon the orientation (related to the direction of the incident wave) and so does the resonance wavelength (cf figures 6(a) and 6(c)). Note that, in this case (resonance of the z-component), there is little difference between the images calculated in CH and CD modes (cf figures 6(b) and 6(d)). Finally, it is worth mentioning that similar images were calculated for the scatterers with $\varepsilon_s = 5$ though the field intensity enhancement was smaller in accordance with the dependences shown in figure 2(a).

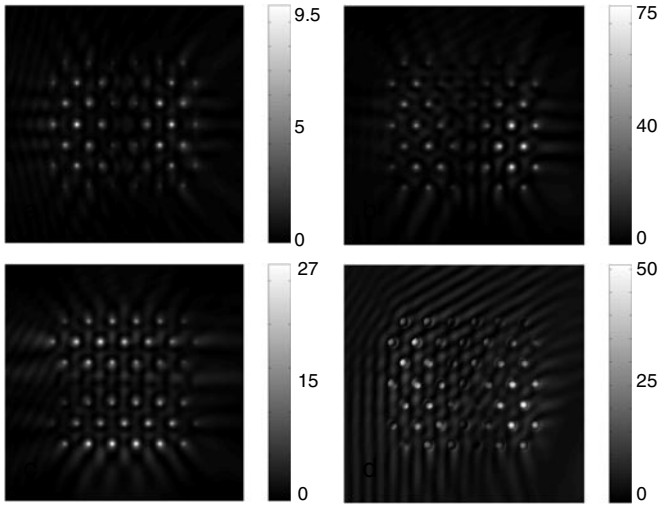

Figure 6. Linear grey-scale representations (6×6 μm^2) of the field (λ = (a), (b) 586 and (c), (d) 588.4 nm) intensity calculated (a)–(c) at the constant height of 211 nm from the substrate surface and (d) at the site of the probe sphere for a p-polarized wave incident at ϕ = (a) 0°, (b), (d) 30° and (c) 45°.

In addition to the resonance peaks considered above, a broad maximum centred at ~606 nm is seen on the wavelength dependences calculated for $\phi = 30°$. This maximum is present for both dielectric constants of scatterers (figure 2(a)) and in a large range of radii (figure 3(c)). The corresponding intensity distributions indicate that, in this case, the intensity enhancement is concentrated within a single hexagonal cluster (figure 7). We believe that this enhancement would survive in some form for the FSPSSSs with different numbers of scatterers. Actually, a rather similar maximum was calculated with a different method and for differently shaped scatterers for the (6×6) array (cf figure 2 and figure 4 from [2]). Such a maximum seems to be more interesting from the point of view of practical realization than the resonance peaks because of relaxed tolerances on the sizes of scatterers and light wavelengths used (though at the expense of the sensitivity with respect to the angle ϕ of light incidence in the surface plane).

4. Conclusions

In this paper we analysed light scattering by a hexagonal finite-size array of spherical scatterers placed on the substrate. It was shown that the self-consistent field established in the process of multiple scattering by a FSPSSS can be resonantly enhanced for certain combinations of system parameters, of which the most important ones are the light wavelength and the polarizability of scatterers. The maximum intensities attained at the resonances were found to be four orders

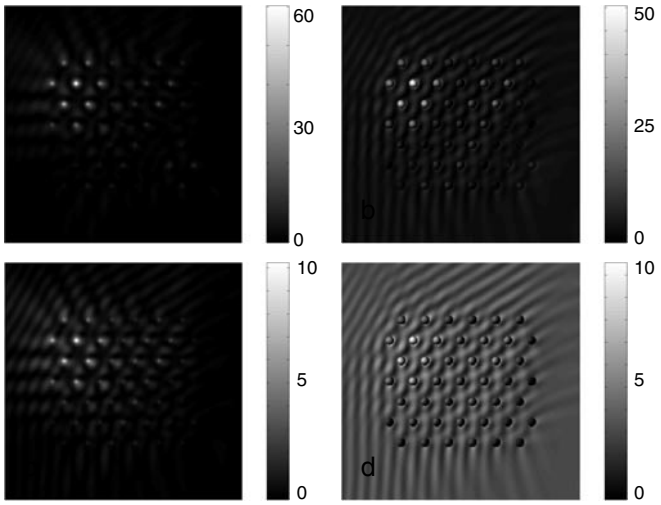

Figure 7. Linear grey-scale representations ($6 \times 6\ \mu m^2$) of the field ($\lambda = 606$ nm) intensity calculated (a), (c) at the constant height of 211 nm from the substrate surface and (b), (d) at the site of the probe sphere with the dielectric constant $\varepsilon_s =$ (a), (b) 10 and (c), (d) 5 for a p-polarized wave incident at $\phi = 30^\circ$.

of magnitude larger than that of the illuminating field below the surface. The intensity field distributions above the scattering system and the near-field optical images simulated in the constant distance mode were presented for the observed resonances.

These results have been obtained in the dipole approximation, but we expect the main conclusions to be valid even when a multipole expansion of the polarizability should be used (for large and/or non-spherical scatterers). The limit of the validity of point dipole approximation can be estimated by considering the unitary limit of the scattering cross section of an individual pointlike scatterer [10]. For an individual scatterer in free space, the limiting radius of a spherical scatterer is $\sim\lambda 2\pi$, so that the value of 100 nm used here is just on the limit. However, as long as the dipole contribution is dominant in the multipole expansion [11, 12] the interaction driven by dipolar polarizabilities of scatterers would ultimately determine the system resonances (and the resonant field configurations).

The strong field enhancement within a narrow range of wavelengths and polarization selectivity of the observed resonances make the phenomenon of resonant field enhancement by FSPSSSs very attractive for various applications ranging from integrated optic and optoelectronic components to bio- and chemical sensors. Our preliminary calculations for differently framed hexagonal arrays of spherical surface scatterers and with different numbers of scatterers indicate that the resonance for the field component perpendicular to the surface shows up persistently at the wavelengths slightly below 600 nm and so does a diffuse maximum (at the wavelengths slightly above 600 nm) for the angle of incidence in the surface plane $\phi = 30^\circ$. We conduct further investigations in this area.

Acknowledgments

MX acknowledges support from CONACYT 32268E and DGAPA IN102600 and the supercomputer at UNAM.

References

[1] Joannopoulos J D, Meade R D and Winn J N 1995 *Photonic Crystals* (Princeton, NJ: Princeton University Press)

[2] Martin O J F, Girard C, Smith D R and Schultz S 1999 Generalized field propagator for arbitrary finite-size photonic band gap structures *Phys. Rev. Lett.* **82** 315–18

[3] Girard C and Dereux A 1996 Near-field optics theories *Rep. Prog. Phys.* **59** 657–99

[4] Shalaev V 1996 Electromagnetic properties of small-particle composites *Phys. Rep.* **272** 61–137

[5] Keller O, Xiao M and Bozhevolnyi S 1993 Configurational resonances in optical near-field microscopy: a rigorous point-dipole approach *Surf. Sci.* **280** 217–30

[6] Kreibig U and Vollmer M 1995 *Optical Properties of Metal Clusters* (Berlin: Springer)

[7] Xiao M 1997 Theoretical treatment for scattering scanning near-field optical microscopy *J. Opt. Soc. Am.* A **14** 2977–84

Bozhevolnyi S I, Xiao M and Hvam J M 1999 Polarization-resolved imaging with a reflection near-field optical microscope *J. Opt. Soc. Am.* A **16** 2649–57

[8] Li Z, Gu B and Yang G 1997 Modified self-consistent approach applied in near-field optics for mesoscopic surface defects *Phys. Rev.* B **55** 10 883–94

[9] Bozhevolnyi S I 1999 Near-field optical microscopy of localized excitations on rough surfaces: influence of a probe *J. Microsc.* **194** 561–6

[10] de Vries P, van Coevorden D V and Lagendijk A 1998 Point scatterers for classical waves *Rev. Mod. Phys.* **70** 447–66

[11] Chaumet P C, Rahmani A, de Fornel F and Dufour J-P 1998 Evanescent light scattering: the validity of the dipole approximation *Phys. Rev.* B **58** 2310–15

[12] Quinten M, Pack A and Wannemacher R 1999 Scattering and extinction of evanescent waves by small particles *Appl. Phys.* B **68** 87–92